Single-Molecule Kinetic Theory of Heterogeneous and Enzyme Catalysis

ARTICLE *in* THE JOURNAL OF PHYSICAL CHEMISTRY C · JANUARY 2009

Impact Factor: 4.77 · DOI: 10.1021/jp808240c

THE JOURNAL OF PHYSICAL CHEMISTRY C

Article

Single-Molecule Kinetic Theory of Heterogeneous and Enzyme Catalysis

Weilin Xu, Jason S. Kong, and Peng Chen

J. Phys. Chem. C, **2009**, 113 (6), 2393-2404 • DOI: 10.1021/jp808240c • Publication Date (Web): 15 January 2009

Single-Molecule Kinetic Theory of Heterogeneous and Enzyme Catalysis

Weilin Xu, Jason S. Kong, and Peng Chen*

Department of Chemistry and Chemical Biology, Cornell University, Ithaca, New York 14853

Received: September 16, 2008; Revised Manuscript Received: November 4, 2008

Recent experimental advances in single-molecule enzymology stimulated many efforts to develop single-molecule kinetic theories of enzyme catalysis, especially for the classic Michaelis−Menten mechanism. Our group recently studied redox catalysis by single metal nanoparticles at single-turnover resolution. Compared with enzymes, which are homogeneous catalysts and have well-defined active sites, nanoparticles are heterogeneous catalysts and have many different surface sites for catalysis. To provide a theoretical framework to understand nanoparticle catalysis at the single-molecule level, here we formulate in detail the single-molecule kinetic theory of a Langmuir−Hinshelwood mechanism for heterogeneous catalysis, which includes the multitude of surface sites on one nanoparticle. We consider two parallel product dissociation pathways that give complex single-molecule kinetics of the product dissociation reaction. We derive the probability density functions of the stochastic waiting times for both the product formation and the product dissociation reactions and describe their complex behaviors at different kinetic limiting conditions. We also obtain a single-molecule Langmuir−Hinshelwood equation that describes the saturation kinetics of the product formation rate over substrate concentrations and evaluate the randomness parameter of single-turnover waiting times. We further compare the single-molecule kinetics between the Langmuir−Hinshelwood mechanism for heterogeneous catalysis and the Michaelis−Menten mechanism for enzyme catalysis and formulate the modified single-molecule Michaelis−Menten kinetics with multiple product dissociation pathways. In the end, we suggest that the Langmuir−Hinshelwood mechanism is also applicable to describe the single-molecule kinetics of oligomeric enzymes that contain multiple catalytic sites. We expect that these theories will enable quantitative analysis of single-turnover kinetics of heterogeneous and enzyme catalysis and provide a theoretical foundation to understand the catalytic dynamics of nanoparticles and enzymes at the single-molecule level.

I. Introduction

Chemical kinetics is powerful to determine the catalytic mechanisms of enzymes, small-molecule catalysts, and heterogeneous catalysts. By examining the catalytic reaction rate across various reaction conditions, one can apply rate laws of chemical kinetics and formulate kinetic mechanisms to gain quantitative understanding of the catalysis. Traditionally, to determine a catalytic reaction rate (v) in ensemble experiments, one measures the time rate of the concentration change of a substrate or a product during catalysis. Well-established ensemble kinetic equations for various reaction mechanisms can then be used to analyze the dependence of v on a reaction condition, such as the substrate concentration [S], to formulate a working mechanism for the catalysis and quantify the associated kinetic parameters.[1,2]

More recently, advances in single-molecule techniques, including single-molecule fluorescence microscopy, made it possible to monitor the catalytic reactions of enzymes,[3−25] microcrystals,[26] and nanoparticles[27] at the single-molecule level. Instead of monitoring the concentration change of the substrate or the product to measure the reaction rate, a single-molecule experiment follows individual catalytic turnovers in real time and records the waiting times (τ) for completing individual reactions. While the individual values of τ are stochastic, its probability distribution and associated statistical properties are defined by the underlying catalytic mechanism and the associated kinetic parameters. Single-molecule kinetic theories have thus been developed to derive and analyze the probability density function $f(\tau)$ of τ and its statistical properties, including the reciprocal of its mean, $\langle\tau\rangle^{-1}$, and its randomness parameter r (defined as $r = (\langle\tau^2\rangle - \langle\tau\rangle^2)/\langle\tau\rangle^2$, where $\langle\ \rangle$ denotes averaging), to probe the catalytic mechanism and quantify the kinetic parameters.[3,4,27−42]

SCHEME 1: Michaelis−Menten Mechanism for Enzyme Catalysis[a]

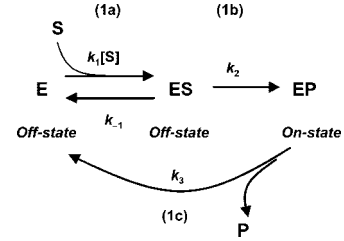

[a] Fluorescence off- and on-states are denoted at each reaction stage for a fluorogenic enzymatic reaction.

Among single-molecule studies of catalysis, enzyme catalysis has been studied most.[3−25] Consequently, single-molecule kinetic theory has been formulated for the classic Michaelis−Menten mechanism in enzyme catalysis,[3,28−38,41,43] and most recently, for generic complex single-molecule kinetic processes.[44] In the classic Michaelis−Menten mechanism (Scheme 1), a substrate S binds reversibly to an enzyme E to form an enzyme−substrate complex ES before being converted to the product P (reactions 1a and 1b); the product then dissociates to regenerate E for the next turnover (reaction 1c, Scheme 1). Associated with reactions

* To whom correspondence should be addressed. E-mail: pc252@cornell.edu.

10.1021/jp808240c CCC: $40.75
Published on Web 01/15/2009

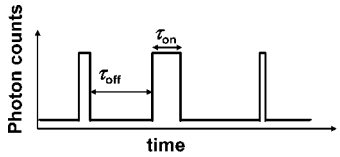

Figure 1. Schematic single-molecule turnover trajectory showing off-on bursts of product formation.

1a and 1b and under steady-state approximation, the classic Michaelis−Menten equation

$$v = \frac{v_{max}[S]}{K_M + [S]} \quad (1)$$

describes the substrate concentration dependence of the ensemble product formation rate v, which increases with increasing [S] and eventually saturates to v_{max}.[1] v_{max} is equal to $k_2[E]_T$, where $[E]_T$ is the total concentration of the enzyme, and K_M (= $(k_{-1} + k_2)/k_1$) is the Michaelis constant and corresponds to the substrate concentration at which $v = v_{max}/2$. In contrast, in single enzyme measurements, the concentration of an enzyme is meaningless; instead, an enzyme molecule has a certain probability at each of the states E, ES, and EP at any time and cycles through these states repetitively. The reaction rate is described by the statistical properties of the stochastic waiting times for completing individual catalytic turnovers.

As an example, consider the experiment of single-molecule detection of a fluorogenic enzyme reaction that operates by the Michaelis−Menten mechanism in Scheme 1. Here an enzyme catalyzes the conversion of a nonfluorescent substrate to a fluorescent product, and the product fluorescence is detected one molecule at a time in real time. Under constant laser illumination during catalysis and detected at longer than μs timescales, the fluorogenic reactions of an enzyme will give stochastic off-on burst-like fluorescence signals (Figure 1); each intensity increase marks a formation of EP, each decrease marks a dissociation of EP (free P diffuses away fast from the detection volume), and each off-on cycle reports a single turnover. τ_{off} is then the waiting time for completing reactions 1a and 1b; τ_{on} is the waiting time for completing reaction 1c; and these two stochastic quantities are the most important observables in a single-turnover trajectory and can be characterized by their probability density functions $f_{off}(\tau)$ and $f_{on}(\tau)$. It was shown that the probability density function of τ_{off}, $f_{off}(\tau)$, is[3,28,31]

$$f_{off}(\tau) = \frac{k_1 k_2[S]}{2a}[e^{(b+a)\tau} - e^{(b-a)\tau}] \quad (2)$$

where $a =$

$$\sqrt{\frac{1}{4}(k_1[S] + k_{-1} + k_2)^2 - k_1 k_2[S]}$$

and $b = -(k_1[S] + k_{-1} + k_2)/2$. The functional shape of $f_{off}(\tau)$ has an exponential rise followed by an exponential decay (Figure 2A); its delayed maximum at $\tau > 0$ indicates the presence of the reaction intermediate ES. The reciprocal of the first moment of $f_{off}(\tau)$, $\langle\tau_{off}\rangle^{-1}$, represents the rate of the product formation. With $\langle\tau_{off}\rangle = \int_0^\infty \tau f_{off}(\tau)d\tau$, it follows:

$$\langle\tau_{off}\rangle^{-1} = \frac{k_2[S]}{[S] + K_M} \quad (3)$$

where $K_M = (k_{-1} + k_2)/k_1$. Equation 3 resembles the ensemble Michaelis−Menten equation (eq 1) and predicts the same hyperbolic dependence of the product formation rate on the substrate concentration (Figure 2B) and, thus, was termed the single-molecule Michaelis−Menten equation by Xie and co-workers.[28]

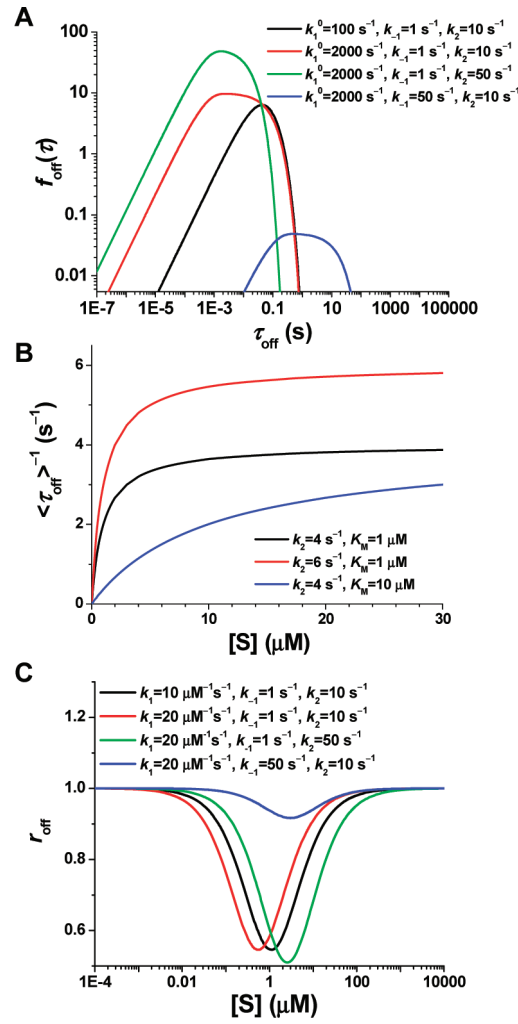

Figure 2. $f_{off}(\tau)$, $\langle\tau_{off}\rangle^{-1}$, and r_{off} of the Michaelis−Menten mechanism. (A) Simulations of $f_{off}(\tau)$ from eq 2 ($k_1^0 = k_1[S]$). (B) Simulations of the [S] dependence of $\langle\tau_{off}\rangle^{-1}$ from eq 3. (C) Simulations of the randomness parameter r_{off} from eq 4.

The randomness parameter for τ_{off}, r_{off}, is a dimensionless measure of the temporal irregularities of τ_{off} and is related to the second moment of $f_{off}(\tau)$:[28,45−47]

$$r_{off} = \frac{\langle\tau_{off}^2\rangle - \langle\tau_{off}\rangle^2}{\langle\tau_{off}\rangle^2} = \frac{(k_1[S] + k_{-1} + k_2)^2 - 2k_1k_2[S]}{(k_1[S] + k_{-1} + k_2)^2} \quad (4)$$

$r_{off} = 1$ at [S] → 0 or [S] → ∞, and $r_{off} < 1$ at intermediate [S] (Figure 2C). Xie and co-workers used serial Poisson processes to illustrate the behavior of r_{off}:[28,31] For a one-step Poisson process with a rate constant k, $f(\tau) = ke^{-k\tau}$, $\langle\tau\rangle = 1/k$, and $\langle\tau^2\rangle - \langle\tau\rangle^2 = 1/k^2$; then $r = 1$. For a serial of n Poisson processes of which every step has the same rate constant k, that is, a complex reaction with n equivalent rate-limiting steps, $f(\tau) = k^n\tau^{n-1}e^{-k\tau}/(n-1)!$; then $\langle\tau\rangle = n/k$ and $\langle\tau^2\rangle - \langle\tau\rangle^2 = n/k^2$; thus, $r = 1/n$. The more rate-limiting steps there are, the smaller r is. In general, $0 < r < 1$ for serial reactions, and its value reflects the number of rate-limiting steps in the reactions. For the Michaelis−Menten mechanism in Scheme 1, at [S] → 0 or [S] → ∞, the τ_{off} reactions only contain one rate-limiting step: substrate binding or catalytic conversion, respectively; then $r_{off} = 1$. At intermediate [S],

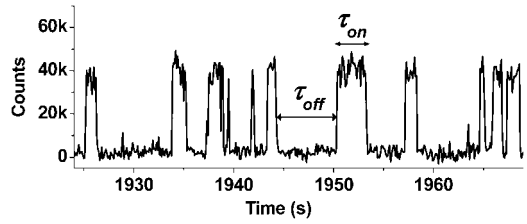

Figure 3. Segment of a single-turnover trajectory of fluorogenic redox catalysis by a single colloidal gold nanoparticle. Figure adapted from Xu et al.[27]

the substrate binding and the catalytic conversion are both rate-limiting; then $r_{off} < 1$, which indicates the presence of the intermediate ES.

For τ_{on}, which contains the unimolecular product dissociation reaction, its probability density function is $f_{on}(\tau) = k_3 e^{-k_3\tau}$, a simple single-exponential decay function with a fixed decay constant k_3; and $\langle\tau_{on}\rangle^{-1} = k_3$, representing the rate of product dissociation. The randomness parameter for τ_{on}, r_{on}, is always unity, because the τ_{on} reaction is a one-step Poisson process.[28,45−47] The overall turnover rate $\langle\tau_{off} + \tau_{on}\rangle^{-1}$ for the enzyme catalysis in Scheme 1 is then $\langle\tau_{off} + \tau_{on}\rangle^{-1} = k_2k_3[S] / [(k_2 + k_3)[S] + k_3K_M]$, which reduces to eq 3, the single-molecule Michaelis−Menten equation, when the product dissociation is fast (i.e., $k_3 \gg k_2$). As the Michaelis−Menten mechanism describes the kinetic behaviors of a large number of enzymes, the above formalism has been particularly useful in analyzing the single-molecule kinetics of enzymatic reactions.[3,4,7,9]

Recently, our group used single-molecule detection of fluorogenic reactions to follow the redox catalysis by single metal nanoparticles in an aqueous environment.[27] By detecting the fluorescence of the catalytic product at the single-molecule level, we recorded real-time single-turnover trajectories of single colloidal gold nanoparticles exhibiting stochastic off-on signals (Figure 3). Compared with enzymes, which are homogeneous catalysts and catalyze reactions at a well-defined active site, nanoparticles are heterogeneous catalysts and have many surface sites for catalysis.[48−50] The one-site, one-substrate model as in the Michaelis−Menten mechanism is thus inadequate for single nanoparticle catalysis, and a Langmuir−Hinshelwood mechanism for heterogeneous catalysis,[51] which considers the multitude of surface sites on one nanoparticle, was used to interpret the single-turnover kinetics of the catalytic product formation reaction by a single nanoparticle. Our single-nanoparticle studies further identified two parallel product dissociation pathways, and between these two pathways, different nanoparticles have differential reactivity giving rise to their heterogeneous kinetics in product dissociation. In this paper, we formulate in detail the single-molecule kinetic theory of the Langmuir−Hinshelwood mechanism for the catalytic product formation reaction and of the product dissociation reaction comprising multiple pathways. We will describe the different behaviors of $f(\tau)$, $\langle\tau\rangle^{-1}$, and r under different kinetic conditions. We will compare the single-molecule kinetics between the Langmuir−Hinshelwood mechanism for heterogeneous catalysis and the Michaelis−Menten mechanism for enzyme catalysis, and formulate the modified single-molecule Michaelis−Menten kinetics containing multiple product dissociation pathways. In the end, we propose that the Langmuir−Hinshelwood mechanism is also applicable to describe the single-molecule kinetics of oligomeric enzymes that have multiple active sites. We expect that the formulism developed here will enable quantitative analysis of single-turnover kinetics of heterogeneous and enzyme catalysis and provide a theoretical foundation to understand the catalytic dynamics of nanoparticles and enzymes at the single-molecule level.

SCHEME 2: Langmuir–Hinshelwood Mechanism with Two Product Dissociation Pathways for Heterogeneous Catalysis[a]

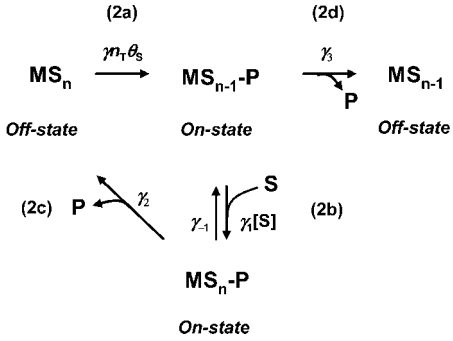

[a] M represents a nanoparticle. n is the number of substrate molecules adsorbed on the nanoparticle surface. n_T is the total number of catalytic sites on one nanoparticle. θ_S is the fraction of the occupied surface catalytic sites by the substrate. γ's are the rate constants. Fluorescence off- and on-states are denoted at each reaction stage for a fluorogenic reaction.

II. Single-Molecule Kinetic Theory of Heterogeneous Catalysis

Scheme 2 shows the kinetic mechanism for a catalytic redox reaction by colloidal gold nanoparticles.[27] The catalytic product formation reaction takes a Langmuir−Hinshelwood mechanism, in which the nanoparticle catalyzes the substrate conversion to product while maintaining a fast substrate adsorption equilibrium (reaction 2a). After being generated, the product can either dissociate via a substrate-assisted pathway, involving a presubstrate-binding step (reactions 2b and 2c), or dissociate directly (reaction 2d). The fluorescence state (off or on) is indicated at each reaction stage. (Note that under the laser excitation intensities in obtaining the data in Figure 3, photobleaching and blinking of the fluorescent product do not affect significantly the duration of the on-times.[27]) In the following, we will formulate in detail the single-molecule kinetics associated with this mechanism.

II.1. τ_{off} Reaction: Langmuir−Hinshelwood Mechanism for Product Formation. ***II.1.A. Probability Density Function $f_{off}(\tau)$.*** The Langmuir−Hinshelwood mechanism assumes that the substrate molecules bind to the nanoparticle surface reversibly and a fast adsorption equilibrium is established at all times (i.e., the rate of substrate adsorption and desorption are much faster than that of the catalytic conversion reaction), and that the surface coverage of substrate molecules on one nanoparticle is governed by the Langmuir adsorption isotherm.[51] Based on this mechanism, the reaction that takes place during the off-times of a single-turnover trajectory of fluorogenic reactions (Figure 3) is reaction 2a in Scheme 2:

$$\underset{\text{off-state}}{MS_n} \xrightarrow{\gamma_{app}} \underset{\text{on-state}}{MS_{n-1} - P} \tag{5}$$

Here n is the number of substrate molecules adsorbed on the nanoparticle surface at equilibrium; γ_{app} is the apparent rate constant for forming one product on the surface of one nanoparticle and takes the form[51]

$$\gamma_{app} = \gamma n \tag{6}$$

where γ is the rate constant representing the intrinsic reactivity per catalytic site for the catalytic conversion reaction. From the Langmuir adsorption isotherm,[51]

$$n = n_T\theta_S = n_T\frac{G_1[S]}{1+G_1[S]} \quad (7)$$

where n_T is the total number of the surface catalytic sites on one nanoparticle, θ_S is the fraction of the occupied surface catalytic sites by the substrate, and G_1 is the substrate adsorption equilibrium constant that equals the ratio of substrate binding and unbinding rate constants. Then we have

$$\gamma_{app} = \gamma n_T\theta_S = \frac{\gamma n_T G_1[S]}{1+G_1[S]} \quad (8)$$

In ensemble measurements where the catalysis by many nanoparticles is measured altogether in solution, the kinetic rate equation for the reaction in eq 5 is

$$\frac{d[MS_{n-1}-P]}{dt} = -\frac{d[MS_n]}{dt} = \gamma_{app}[MS_n] \quad (9)$$

where M represents a nanoparticle, $[MS_n]$ is the concentration of nanoparticles that do not carry any product, and $[MS_{n-1} - P]$ is the concentration of nanoparticles on which one product molecule is generated. The approximation of γ_{app} as a pseudofirst-order rate constant here is valid, provided [S] is time-independent (see below).

In single-turnover measurements of single-nanoparticle catalysis, although the concentration of the substrate, [S], is still a valid description, the concentration of one nanoparticle is meaningless, and each nanoparticle has a certain probability at either the MS_n or the $MS_{n-1} - P$ state during an off-time. To derive the single-molecule kinetics for a single nanoparticle, the concentrations in eq 9 need to be replaced by the probabilities $P(t)$ of finding the nanoparticle in the states MS_n and $MS_{n-1} - P$ at time t.[31] Then, we have

$$\frac{dP_{MS_{n-1}-P}(t)}{dt} = -\frac{dP_{MS_n}(t)}{dt} = \gamma_{app}P_{MS_n}(t) \quad (10)$$

where $P_{MS_n}(t) + P_{MS_{n-1}-P}(t) = 1$. At the onset of each off-time reaction ($t = 0$), no product molecule has formed. So the initial conditions for solving eq 10 are $P_{MS_n}(0) = 1$ and $P_{MS_{n-1}-P}(0) = 0$. In single-nanoparticle experiments, the depletion of substrate is negligible during catalysis and [S] is time-independent; γ_{app} can thus be validly taken as a pseudofirst-order rate constant.

We can then evaluate the probability density of the time τ needed to complete the off-time reaction, $f_{off}(\tau)$, that is, the probability density of τ_{off}. The probability of finding a particular τ is $f_{off}(\tau)\Delta\tau$; and $f_{off}(\tau)\Delta\tau$ is equal to the probability for the nanoparticle to switch from the MS_n state to the $MS_{n-1} - P$ state between $t = \tau$ and $\tau + \Delta\tau$, which is $\Delta P_{MS_{n-1}-P}(\tau) = \gamma_{app}P_{MS_n}(\tau)\Delta\tau$. In the limit of infinitesimal $\Delta\tau$,

$$f_{off}(\tau) = \frac{dP_{MS_{n-1}-P}(\tau)}{d\tau} = \gamma_{app}P_{MS_n}(\tau) = \frac{\gamma n_T G_1[S]}{1+G_1[S]}P_{MS_n}(\tau) \quad (11)$$

Solving eq 10 for $P_{MS_n}(\tau)$, we get

$$f_{off}(\tau) = \frac{\gamma n_T G_1[S]}{1+G_1[S]}\exp\left(-\frac{\gamma n_T G_1[S]}{1+G_1[S]}\tau\right) \quad (12)$$

Clearly, regardless of the values of γ, n_T, or G_1, $f_{off}(\tau)$ will show a single-exponential decay with the [S]-dependent decay constant $\gamma n_T G_1[S]/(1 + G_1[S])$. At saturating substrate concentrations where all surface catalytic sites are occupied by substrates, $\theta_S = 1$ and $f_{off}(\tau) = \gamma n_T \exp(-\gamma n_T\tau)$. Figure 4A plots $f_{off}(\tau)$ at different values of γn_T, [S], and G_1. Figure 4B shows the experimental distribution of τ_{off} from a single-turnover trajectory of gold nanoparticle catalysis at a saturating substrate

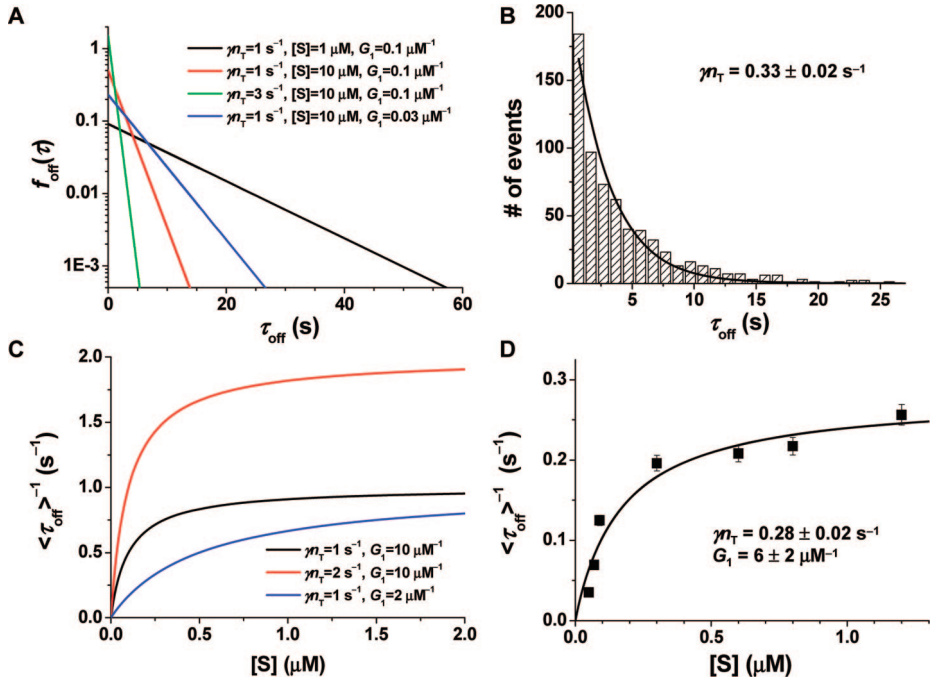

Figure 4. $f_{off}(\tau)$ and $\langle\tau_{off}\rangle^{-1}$ of the Langmuir−Hinshelwood mechanism for the catalytic product formation reaction. (A) Simulations of the probability density function $f_{off}(\tau)$ at different γn_T, [S], and G_1 from eq 12. (B) Experimental τ_{off} distribution from a single-turnover trajectory of gold nanoparticle catalysis at a saturating substrate concentration ([S] = 1.2 μM).[27] Solid line is a single-exponential fit; its decay constant gives γn_T. (C) Simulations of the [S] dependence of $\langle\tau_{off}\rangle^{-1}$ from eq 13 at different γn_T and G_1. (D) Experimental results of the [S] dependence of $\langle\tau_{off}\rangle^{-1}$ of single gold nanoparticle catalysis, where each data point is averaged over many nanoparticles. Data are adapted from Xu et al.[27] Solid line is a fit with eq 13.

concentration;[27] fitting this distribution gives γn_T of this nanoparticle directly.

II.1.B. Rate of Product Formation: $\langle \tau_{off} \rangle^{-1}$**.** The first moment of $f_{off}(\tau)$, $\langle \tau_{off} \rangle = \int_0^\infty \tau f_{off}(\tau)\, d\tau$, gives the mean waiting time for completing the catalytic product formation reaction; $\langle \tau_{off} \rangle^{-1}$ then represents the rate of product formation for a single nanoparticle:

$$\langle \tau_{off} \rangle^{-1} = \frac{\gamma n_T G_1[S]}{1 + G_1[S]} \tag{13}$$

This equation resembles the ensemble Langmuir−Hinshelwood rate equation;[51] we thus call it single-molecule Langmuir−Hinshelwood equation. This equation describes the hyperbolic dependence of $\langle \tau_{off} \rangle^{-1}$ on the substrate concentration with a saturation to γn_T at high substrate concentrations. To give a physical interpretation of eq 13: The maximum product formation rate is reached when all surface catalytic sites are occupied by substrates, and the reaction rate $\langle \tau_{off} \rangle^{-1}$ equals the reactivity (γ) per catalytic site multiplied by the total number (n_T) of surface catalytic sites. Figure 4C plots the [S] dependence of $\langle \tau_{off} \rangle^{-1}$ at different values of γn_T and G_1. Figure 4D shows the experimental data of redox catalysis of gold nanoparticles;[27] fitting the data with eq 13 gives γn_T and G_1.

II.1.C. Randomness Parameter r_{off}**.** From eq 13, we can obtain $\langle \tau_{off} \rangle = 1/\gamma_{app}$ and $\langle \tau_{off}^2 \rangle = 2/\gamma_{app}^2$. Then $r_{off} = (\langle \tau_{off}^2 \rangle - \langle \tau_{off} \rangle^2)/\langle \tau_{off} \rangle^2 = 1$, independent of [S]. This is consistent with that $f_{off}(\tau)$ is a single-exponential decay function, which results from that the τ_{off} reaction of the Langmuir−Hinshelwood mechanism only contains one rate-limiting step (Scheme 2 and eq 5), equivalent to a Poisson process.

II.2. τ_{on} Reaction: Two-Pathway Model for Production Dissociation. ***II.2.A. Probability Density Function*** $f_{on}(\tau)$**.** For product dissociation, the mechanism in Scheme 2 includes two parallel pathways: a substrate-assisted pathway involving a presubstrate-binding step before product dissociation (reactions 2b and 2c) and a direct dissociation pathway (reaction 2c). Thus, the reaction taking place during each on-time is either

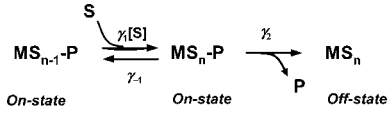

(14a)

or

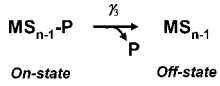

(14b)

Under the assumption of the Langmuir−Hinshelwood mechanism that a fast substrate adsorption equilibrium is established at all times, the MS_{n-1} state will quickly turn to the MS_n state by binding a substrate molecule from the solution. We can show that the probability density function $f_{on}(\tau)$ is (Appendix A)

$$f_{on}(\tau) = \frac{1}{2\alpha}[Me^{(\beta+\alpha)\tau} + Ne^{(\beta-\alpha)\tau}] \tag{15}$$

where $\alpha = \sqrt{(\gamma_1[S]+\gamma_{-1}+\gamma_2+\gamma_3)^2/4-(\gamma_1\gamma_2[S]+\gamma_{-1}\gamma_3+\gamma_2\gamma_3)}$, $\beta = -(\gamma_1[S] + \gamma_{-1} + \gamma_2 + \gamma_3)/2$, $M = \gamma_2\gamma_1[S] + \gamma_3\alpha + \gamma_3\beta + \gamma_3\gamma_{-1} + \gamma_3\gamma_2$, and $N = -\gamma_2\gamma_1[S] + \gamma_3\alpha - \gamma_3\beta - \gamma_3\gamma_{-1} - \gamma_3\gamma_2$.

Depending on the substrate concentration and the magnitudes of the individual rate constants, $f_{on}(\tau)$ will exhibit different shapes. Here we consider $f_{on}(\tau)$ in five limiting regimes. (*i*) Complete shutdown of the substrate-assisted dissociation pathway, that is, $\gamma_1 = \gamma_{-1} = \gamma_2 = 0$. Equation 15 then reduces to $f_{on}(\tau)_{\gamma_1 = \gamma_{-1} = \gamma_2 = 0} = \gamma_3 e^{-\gamma_3 \tau}$, which is a single-exponential decay function with a decay constant γ_3 (Figure 5A). (*ii*) Complete shutdown of the direct dissociation pathway, that is, $\gamma_3 = 0$. Equation 15 then becomes $f_{on}(\tau)_{\gamma_3=0} = (\gamma_1\gamma_2[S]/2\alpha)\,[e^{(\beta+\alpha)\tau} - e^{(\beta-\alpha)\tau}]$, where $\alpha_{\gamma_3=0} = \sqrt{(\gamma_1[S] + \gamma_{-1} + \gamma_2)^2/4 - \gamma_1\gamma_2[S]}$ and $\beta_{\gamma_3=0} = -(\gamma_1[S] + \gamma_{-1} + \gamma_2)/2$. $f_{on}(\tau)_{\gamma_3=0}$ contains two exponentials and shows an exponential rise followed by an exponential decay. Particularly, at $\tau = 0$, $f_{on}(\tau)_{\gamma_3=0} = 0$; this is due to the existence of the kinetic intermediate $MS_n - P$ after the substrate-binding step, which imposes nonzero waiting time for completing product dissociation and leads to the delayed maximum at $\tau > 0$. Figure 5B plots $f_{on}(\tau)_{\gamma_3=0}$ at different $\gamma_1{}^0$ ($= \gamma_1[S]$), γ_{-1}, and γ_2. Depending on the relative magnitudes of these rate constants and on the experimental time resolution, the initial exponential rise of $f_{on}(\tau)_{\gamma_3=0}$ may not be experimentally resolvable. (*iii*) Both dissociation pathways present, but with $\gamma_2 > \gamma_3$. $f_{on}(\tau)$ then still shows an initial rise followed by a decay but with a nonzero probability at $\tau = 0$ ($f_{on}(0) = \gamma_3$) due to the direct dissociation pathway (Figure 5C). However, there is still a delayed maximum at $\tau > 0$, reflecting the presence of the $MS_n - P$ intermediate. Similarly, the initial rise of $f_{on}(\tau)$ here may not be experimentally resolvable depending on the magnitudes of the rate constants. (*iv*) Both dissociation pathways present, but with $\gamma_2 < \gamma_3$. Here as the direct dissociation is always faster than the substrate-assisted one, there is no significant population of the $MS_n - P$ intermediate, and $f_{on}(\tau)$ has no maximum at $\tau > 0$ and contains two exponential decays with the two decay constants being $\beta + \alpha$ and $\beta - \alpha$ (eq 15 and Figure 5C). The magnitude of the difference between $\beta + \alpha$ and $\beta - \alpha$ determines whether these two decay components are experimentally resolvable. (*v*) Both dissociation pathways present, but with $\gamma_2 = \gamma_3$. At this limiting condition, eq 15 becomes $f_{on}(\tau)_{\gamma_2 = \gamma_3} = \gamma_2 e^{-\gamma_2\tau} = \gamma_3 e^{-\gamma_3\tau}$, which exhibits a single-exponential decay (Figure 5C).

Except in regime (*i*), in all other limiting regimes where the substrate-assisted pathway exists for product dissociation, eq 15 will reduce to a single-exponential decay at high substrate concentrations, $f_{on}(\tau)_{[S]\to\infty} \approx \gamma_2 e^{-\gamma_2\tau}$. The high substrate concentration here drives the product dissociation toward the substrate-assisted pathway, making the direct dissociation negligible. Figure 5D shows the experimental distribution of τ_{on} from a single-turnover trajectory of a gold nanoparticle at a saturating substrate concentration; fitting with a single-exponential decay function gives γ_2 for this nanoparticle directly. (For these gold nanoparticles, we did not observe the initial-rise-then-decay nor the double-exponential-decay behaviors of $f_{on}(\tau)$, probably due to large values of γ_1 or γ_{-1} for reaction 2b of the catalysis in Scheme 2.)

II.2.B. Rate of Product Dissociation: $\langle \tau_{on} \rangle^{-1}$**.** From eq 15, we can obtain $\langle \tau_{on} \rangle^{-1}$ ($= 1/\int_0^\infty \tau f_{on}(\tau)\, d\tau$), the single-nanoparticle product dissociation rate:

$$\langle \tau_{on} \rangle^{-1} = \frac{\gamma_2 G_2[S] + \gamma_3}{1 + G_2[S]} \tag{16}$$

where $G_2 = \gamma_1/(\gamma_{-1} + \gamma_2)$. When $[S] \to 0$, $\langle \tau_{on} \rangle_{[S]\to 0}^{-1} = \gamma_3$; When $[S] \to \infty$, $\langle \tau_{on} \rangle_{[S]\to\infty}^{-1} = \gamma_2$. The physical meaning of the limiting values of eq 16 can be understood as follows: When $[S] \to 0$, the forward reaction of reaction 2b is negligible ($\gamma_1[S] = 0$, Scheme 2); then the product dissociation dominantly takes the

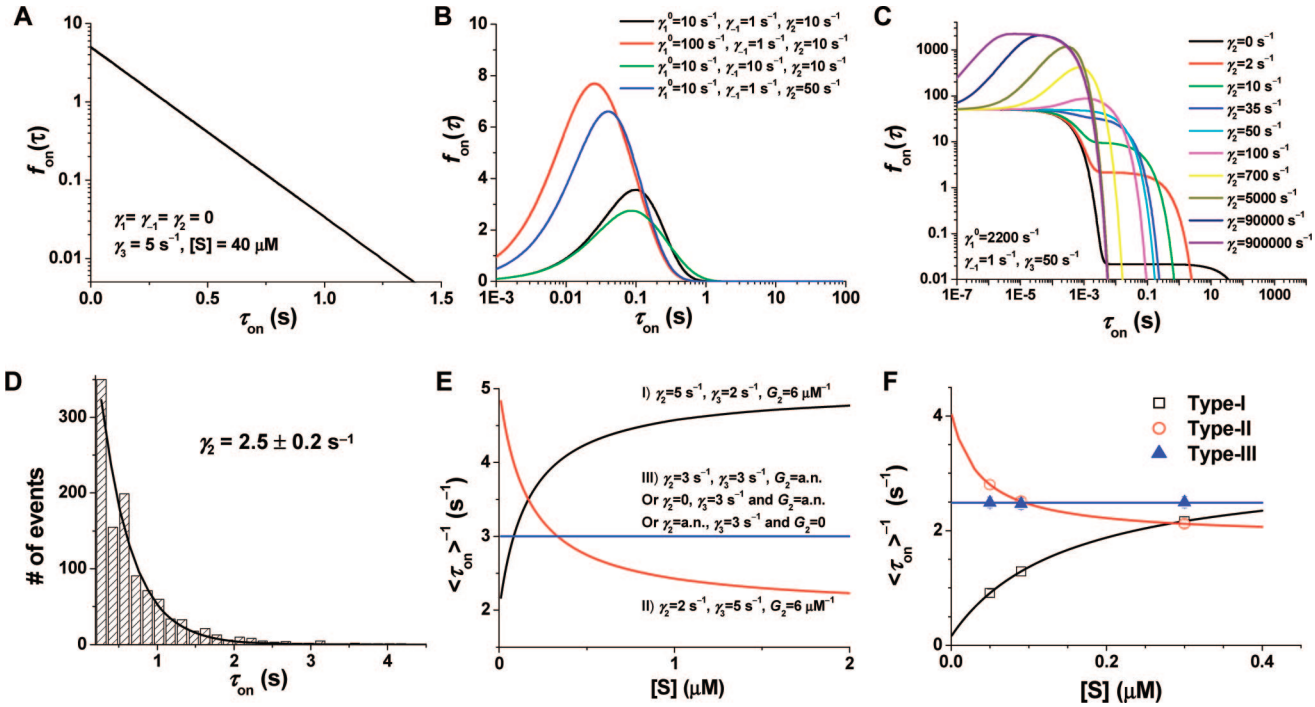

Figure 5. $f_{on}(\tau)$ and $\langle\tau_{on}\rangle^{-1}$ of the Langmuir−Hinshelwood mechanism with two product dissociation pathways. (A) Simulation of the probability density function $f_{on}(\tau)$ from eq 15 in the case of the shutdown of the substrate-assisted dissociation pathway ($\gamma_1 = \gamma_{-1} = \gamma_2 = 0$). (B) Simulations of $f_{on}(\tau)$ from eq 15 in the case of the shutdown of the direct dissociation pathway ($\gamma_3 = 0$; $\gamma_1^0 = \gamma_1[S]$). (C) Simulations of $f_{on}(\tau)$ from eq 15 with varying relative magnitudes of γ_2 and γ_3. (D) Experimental data of a τ_{on} distribution from a single-turnover trajectory of gold nanoparticle catalysis at a saturating substrate concentration ([S] = 1.2 μM).[27] Solid line is an exponential fit; its decay constant gives γ_2. (E) Simulations of the [S] dependence of $\langle\tau_{on}\rangle^{-1}$ from eq 16, showing three different types of behaviors. (a.n. = arbitrary number.) (F) Experimental data of [S] dependence of $\langle\tau_{on}\rangle^{-1}$ from three single gold nanoparticle catalysis trajectories, exemplifying the three types of kinetic behaviors. Solid lines are fits with eq 16. Data adapted from Xu et al.[27]

direct dissociation pathway (reaction 2d) and the reaction rate is determined by γ_3. When [S] → ∞, the MS_{n-1} − P state will be immediately converted to the MS_n − P state via reaction 2b due to the large value of γ_1[S]; then the product dissociation dominantly takes the substrate-assisted pathway and the reaction rate is determined by γ_2 (reaction 2c).

With different relative magnitudes of γ_2 and γ_3, eq 16 predicts three types of [S] dependence of $\langle\tau_{on}\rangle^{-1}$. (I) When $\gamma_2 > \gamma_3$, $\langle\tau_{on}\rangle^{-1}$ will increase with increasing [S] and eventually saturate. (II) When $\gamma_2 < \gamma_3$, $\langle\tau_{on}\rangle^{-1}$ will decrease with increasing [S] and flatten. (III) When $\gamma_2 = \gamma_3$, or $\gamma_1 = 0$ (i.e., $G_2 = 0$) that represents the complete shutdown of the substrate-assisted dissociation pathway, $\langle\tau_{on}\rangle^{-1}$ will be a constant and independent of [S]. Figure 5E plots the three types of [S] dependence of $\langle\tau_{on}\rangle^{-1}$. All these three types of kinetic behaviors were observed experimentally in our study of single gold nanoparticle catalysis (Figure 5F),[27] which exemplifies the heterogeneous catalytic properties of nanoparticle catalysts as well as the ability of single-nanoparticle experiments in revealing them.

II.2.C. Randomness Parameter r_{on}. With $f_{on}(\tau)$, we can get $\langle\tau_{on}\rangle$ and $\langle\tau_{on}^2\rangle$ ($= N/[\alpha(\alpha-\beta)^3] - M/[\alpha(\alpha+\beta)^3]$) to calculate r_{on}. At [S] = 0 or [S] → ∞, $r_{on} = 1$; this is because at these two limiting conditions $f_{on}(\tau)$ is a single-exponential decay function. At intermediate [S] and depending on the relative magnitudes of γ_2 and γ_3, r_{on} has three different ranges of values that are directly related to the functional shapes of $f_{on}(\tau)$ (Figure 6):

(*i*) When $\gamma_2 = \gamma_3$, $r_{on} = 1$. This directly results from that at this condition $f_{on}(\tau)$ is always a single-exponential decay function (Figure 5C).

(*ii*) When $\gamma_2 > \gamma_3$, $r_{on} < 1$. This comes from that $f_{on}(\tau)$ here contains two exponential functions connected by a minus sign (eq 15), which gives its exponential-rise-followed-by-exponential-decay behavior with a delayed maximum that indicates the presence of the MS_n − P intermediate (Figure 5C). The relation between the functional shape of $f_{on}(\tau)$ and the value of r_{on} here can be illustrated by considering the general probability density function $f(\tau) = c_1k_1e^{-k_1\tau} - c_2k_2e^{-k_2\tau}$, where the coefficients c_1 and c_2 are both positive and $c_1 - c_2 = 1$ from the normalization condition $\int_0^\infty f(\tau)d\tau = 1$. For this $f(\tau)$, $\langle\tau^2\rangle - 2\langle\tau\rangle^2 = -2c_1c_2(k_1-k_2)^2/(k_1^2k_2^2) < 0$ when $k_1 \neq k_2$; therefore, $r = (\langle\tau^2\rangle - \langle\tau\rangle^2)/\langle\tau\rangle^2 < 1$.

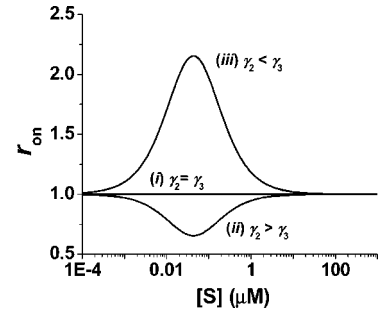

Figure 6. r_{on} for the τ_{on} reaction of the Langmuir−Hinshelwood mechanism (Scheme 2). For all three curves, $\gamma_1 = 300\ \mu M^{-1}\ s^{-1}$ and $\gamma_{-1} = 3\ s^{-1}$. (*i*) $\gamma_2 = \gamma_3 = 10\ s^{-1}$. (*ii*) $\gamma_2 = 10\ s^{-1}$ and $\gamma_3 = 4\ s^{-1}$. (*iii*) $\gamma_2 = 10\ s^{-1}$ and $\gamma_3 = 400\ s^{-1}$.

(*iii*) When $\gamma_2 < \gamma_3$, $r_{on} > 1$. This directly comes from that $f_{on}(\tau)$ here is a double-exponential decay function (Figure 5C), that is, containing two exponential functions connected by a plus sign (eq 15). To illustrate the connection between $f_{on}(\tau)$ and r_{on} here, we can consider the general probability density function $f(\tau) = c_1k_1e^{-k_1\tau} + c_2k_2e^{-k_2\tau}$, where the coefficients c_1 and c_2 are both positive and $c_1 + c_2 = 1$ from the normalization condition $\int_0^\infty f(\tau)\ d\tau = 1$. For this $f(\tau)$, $\langle\tau^2\rangle - 2\langle\tau\rangle^2 = 2c_1c_2$

$(k_1 - k_2)^2 / (k_1^2 k_2^2) > 0$ when $k_1 \neq k_2$; therefore, $r = (\langle\tau^2\rangle - \langle\tau\rangle^2)/\langle\tau\rangle^2 > 1$.

$r_{on} > 1$ here is particularly interesting, as in general $0 < r < 1$ for serial reactions (see Introduction); and only when dynamic disorder is present, $r > 1$.[28,31] Here we show that, if $f(\tau)$ shows double-exponential decay behavior, $r > 1$. The double-exponential decay behavior of $f(\tau)$ can come from many different physical origins, such as parallel reaction pathways in the τ_{on} reaction of nanoparticle catalysis investigated here or dynamic disorder discussed in previous single-molecule Michaelis–Menten kinetics.[28,31] (Note, for the case of parallel reaction pathways, it cannot be that all pathways are simple one-step reactions, which will give $r = 1$ (Appendix C).)

II.3. Overall Turnover Rate. With eqs 13 and 16, we can get the overall turnover rate of the catalysis, $\langle\tau_{off+on}\rangle^{-1}$, that is, the number of turnovers per unit time for a single nanoparticle,

$$\langle\tau_{off+on}\rangle^{-1} = \langle\tau_{off} + \tau_{on}\rangle^{-1} = (\langle\tau_{off}\rangle + \langle\tau_{on}\rangle)^{-1} = \frac{\gamma n_T \gamma_2 G_1 G_2 [S]^2 + \gamma n_T \gamma_3 G_1 [S]}{(\gamma n_T + \gamma_2) G_1 G_2 [S]^2 + (\gamma n_T G_1 + \gamma_3 G_1 + \gamma_2 G_2)[S] + \gamma_3} \quad (17)$$

At $[S] = 0$, $\langle\tau_{off+on}\rangle^{-1}_{[S]=0} = 0$ and no catalysis occurs; at $[S] \rightarrow \infty$, $\langle\tau_{off+on}\rangle^{-1}_{[S]\rightarrow\infty} = \gamma n_T \gamma_2/(\gamma n_T + \gamma_2)$, which reduces to γn_T when the catalytic conversion reaction is rate-limiting in the catalytic cycle (i.e., $\gamma n_T \ll \gamma_2$).

III. Comparison of Heterogeneous and Enzyme Catalysis: Langmuir–Hinshelwood versus Michaelis–Menten Mechanism

For the catalytic product formation reaction contained in τ_{off} of the single-turnover trajectories, both the Michaelis–Menten mechanism and the Langmuir–Hinshelwood mechanism predict the saturation kinetics of the product formation rate $\langle\tau_{off}\rangle^{-1}$ (eqs 3 and 13). The kinetic saturation is due to substrate binding to the catalytic site in both mechanisms, and the maximum reaction rate is reached when the catalytic sites are fully occupied at high substrate concentrations. For the Michaelis–Menten mechanism, $\langle\tau_{off}\rangle^{-1}$ saturates to k_2, the catalytic rate constant, which describes the intrinsic reactivity of a single enzyme (Equation 3); for the Langmuir–Hinshelwood mechanism, $\langle\tau_{off}\rangle^{-1}$ saturates to γn_T, which represents the combined reactivity of all surface catalytic sites of a single nanoparticle (Equation 13).

For the distribution of τ_{off}, $f_{off}(\tau)$, these two mechanisms predict different behaviors. While $f_{off}(\tau)$ of the Michaelis–Menten mechanism has two exponential components, an exponential rise and an exponential decay (eq 2), $f_{off}(\tau)$ of the Langmuir–Hinshelwood mechanism is always a single-exponential decay function with a [S]-dependent decay constant (eq 12). The absence of a second exponential component in $f_{off}(\tau)$ of the Langmuir–Hinshelwood mechanism comes from its presumption that a fast substrate adsorption equilibrium is established at all times during catalysis, that is, substrate adsorption–desorption is much faster than catalysis; thus, the off-time process in the single-turnover trajectories contains only one rate-limiting reaction: the catalytic conversion step (eq 5), leading to the single-exponential decay behavior of $f_{off}(\tau)$. The [S]-dependence of $f_{off}(\tau)$ of the Langmuir–Hinshelwood mechanism results from the multitude of surface catalytic sites, whose occupation is determined by the substrate-concentration and the adsorption equilibrium constant (eq 7). Comparatively, for the Michaelis–Menten mechanism (Scheme 1), if assuming fast substrate binding–unbinding (k_1, $k_{-1} \gg k_2$), $f_{off}(\tau)$ becomes

SCHEME 3: Modified Michaelis–Menten Mechanism with Two Product Dissociation Pathways[a]

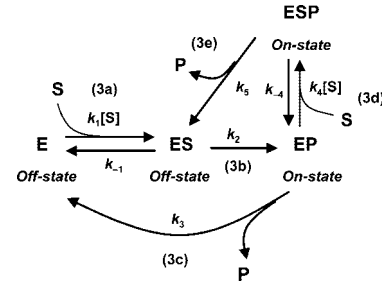

[a] The fluorescence off- and on-states are denoted for a fluorogenic reaction.

$f_{off}(\tau) = [k_1 k_2 [S] / (k_1 [S] + k_{-1} + k_2)] \exp[-k_1 k_2 [S] \tau / (k_1 [S] + k_{-1} + k_2)]$, also a single-exponential decay function with a [S]-dependent decay constant;[28] the [S]-dependence here results from the [S]-controlled availability of the ES intermediate.

The difference in $f_{off}(\tau)$ between the Langmuir–Hinshelwood mechanism and the Michaelis–Menten mechanism leads to their different [S]-dependence of the randomness parameter r_{off}. The single-exponential decay distribution of $f_{off}(\tau)$ of the Langmuir–Hinshelwood mechanism gives $r_{off} = 1$ independent of [S], while for the Michaelis–Menten mechanism, the exponential-rise-followed-by-a-decay behavior of $f_{off}(\tau)$ leads to $r_{off} < 1$ at any [S], except $[S] = 0$ or ∞.

The multitude of surface sites of the nanoparticle can play important roles in their heterogeneous catalytic properties. Our recent study of single gold nanoparticle catalysis revealed both static and dynamic activity heterogeneity, that is, static and dynamic disorder of activity, among nanoparticles with a narrow size dispersion.[27] The explicit inclusion of the number of catalytic sites on the nanoparticle in the single-molecule Langmuir–Hinshelwood kinetics offers an additional factor to account for these heterogeneous single-turnover kinetics (for example, heterogeneity in the number of surface sites), besides the heterogeneity in the intrinsic activity per surface site.

IV. Michaelis–Menten Mechanism Coupled with Multiple Product Dissociation Pathways

The Langmuir–Hinshelwood mechanism in Scheme 2 includes a substrate-assisted product dissociation pathway besides the direct dissociation pathway, whereas the classic Michaelis–Menten mechanism in Scheme 1 only has a direct product dissociation pathway. The substrate-assisted product dissociation is also relevant for enzyme catalysis, however, such as for the catalysis of farnesyltransferase and geranylgeranyltransferase.[52–54] To probe the effect of multiple product dissociation pathways on the single-molecule kinetics of enzyme catalysis, here we consider a modified Michaelis–Menten mechanism incorporating an additional substrate-assisted pathway for product dissociation (Scheme 3).

IV.1. τ_{on} Reaction of the Modified Michaelis–Menten Mechanism. Here we consider first the on-time process in a single-turnover trajectory, as it exactly parallels the treatment of the on-time for the Langmuir–Hinshelwood mechanism in Scheme 2. The reactions occurring in the on-times are either reaction 3c or reactions 3d and 3e. Following the same procedures as in Section II.2, the distribution of τ_{on} for the modified Michaelis–Menten mechanism is

$$f_{on}(\tau) = \frac{1}{2c}[Pe^{(d+c)\tau} + Qe^{(d-c)\tau}] \quad (18)$$

with $c = \sqrt{(k_4[S]+k_{-4}+k_5+k_3)^2/4-(k_4k_5[S]+k_{-4}k_3+k_5k_3)}$, $d = -(k_4[S] + k_{-4} + k_5 + k_3)/2$, $P = k_5k_4[S] + k_3c + k_3d + k_3k_{-4} + k_3k_5$, and $Q = -k_5k_4[S] + k_3c - k_3d - k_3k_{-4} - k_3k_5$. And

$$\langle\tau_{on}\rangle^{-1} = \frac{k_5K_2[S]+k_3}{1+K_2[S]} \quad (19)$$

where $K_2 = k_4/(k_{-4} + k_5)$. Depending on the relative magnitudes of k_3 and k_5, which will give different functional shapes of $f_{on}(\tau)$, the randomness parameter r_{on} here will have three different ranges of values, as discussed in Section II.2.C.

IV.2. τ_{off} Reaction of the Modified Michaelis−Menten Mechanism. ***IV.2.A. Probability Density Function $f_{off}(\tau)$.*** For the off-time process, the relevant reactions are 3a and 3b. Because of the presence of two product dissociation pathways, two sets of initial conditions are possible at the onset of each off-time reaction: (*i*) $P_E(0) = 1$ and $P_{ES}(0) = P_{EP}(0) = 0$, if the product takes the direct dissociation pathway (reaction 3c, Scheme 3); or (*ii*) $P_E(0) = P_{EP}(0) = 0$ and $P_{ES}(0) = 1$, if the product takes the substrate-assisted dissociation pathway (reactions 3d and 3e). With the first set of initial conditions, the τ_{off} probability density function is (Appendix B):

$$f_{off}(\tau)_1 = \frac{k_1k_2[S]}{2a}[e^{(b+a)\tau} - e^{(b-a)\tau}] \quad (20)$$

with $a = \sqrt{(k_1[S]+k_{-1}+k_2)^2/4-k_1k_2[S]}$ and $b = -(k_1[S] + k_{-1} + k_2)/2$. This equation is the same as eq 2. With the second set of initial conditions, we get (Appendix B):

$$f_{off}(\tau)_2 = \frac{k_2}{2a}[(a+b+k_1[S])e^{(b+a)\tau} + (a-b-k_1[S])e^{(b-a)\tau}] \quad (21)$$

with the same a and b as above. Because both sets of initial conditions are possible, the probability density of τ_{off} should overall be a linear combination of eqs 20 and 21 for the modified Michaelis−Menten mechanism:

$$f_{off}(\tau) = C_1f_{off}(\tau)_1 + C_2f_{off}(\tau)_2 \quad (22)$$

Here C_1 and C_2 are two normalized weight coefficients representing the likelihoods of the two initial conditions, that is, the likelihood of the product taking the direct dissociation pathway or that of taking the substrate-assisted pathway. Considering the relative rates for the product to take these two dissociation pathways, we get (Appendix B)

$$C_1 = \frac{k_3(1+K_2[S])}{k_5K_2[S]+k_3(1+K_2[S])} \quad (23a)$$

$$C_2 = \frac{k_5K_2[S]}{k_5K_2[S]+k_3(1+K_2[S])} \quad (23b)$$

To describe the behavior of $f_{off}(\tau)$ for the modified Michaelis−Menten mechanism, we consider it in three different regimes:

(*i*) $C_1 = 1$ and $C_2 = 0$ (e.g., k_4 or $k_5 = 0$). This limiting case corresponds to the sole presence of the direct dissociation pathway, that is, the absence of the substrate-assisted pathway for product dissociation. $f_{off}(\tau)$ then reduces to $f_{off}(\tau)_1$ (eq 20), equivalent to that of the normal Michaelis−Menten mechanism, and has an exponential rise followed by an exponential decay (Figure 7A). Here the delayed maximum of $f_{off}(\tau)$ at $\tau > 0$ indicates the population of the reaction intermediate ES during reaction.

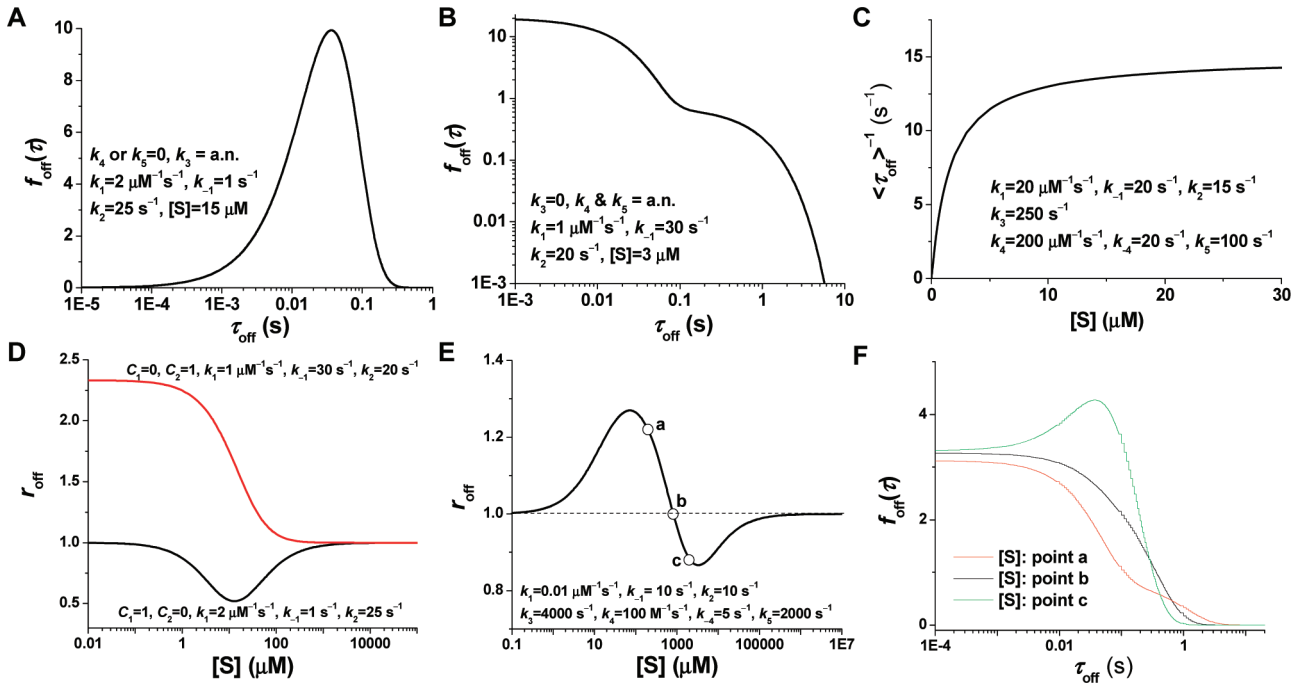

Figure 7. $f_{off}(\tau)$, $\langle\tau_{off}\rangle^{-1}$, and r_{off} for the modified Michaelis−Menten mechanism with two parallel product dissociation pathways. (A) Simulation of $f_{off}(\tau)$ from eq 22 at the condition of $C_1 = 1$ and $C_2 = 0$, corresponding to the sole presence of the direct dissociation pathway. (B) Simulation of $f_{off}(\tau)$ from eq 22 at the condition of $C_1 = 0$ and $C_2 = 1$, corresponding to the sole presence of the substrate-assisted dissociation pathway. (C) Simulation of $\langle\tau_{off}\rangle^{-1}$ from eq 25. (D) Simulation of r_{off} with $C_1 = 1$, $C_2 = 0$, and with $C_1 = 0$, $C_2 = 1$. (E) Simulation of r_{off} with $C_1 \neq 0$ and $C_2 \neq 0$. (F) Three $f_{off}(\tau)$ corresponding to points a, b, and c in (E).

(*ii*) $C_1 = 0$ and $C_2 = 1$ (e.g., $k_3 = 0$). This limiting case corresponds to the sole presence of the substrate-assisted dissociation pathway, that is, the absence of the direct product dissociation pathway. $f_{off}(\tau)$ then reduces to $f_{off}(\tau)_2$ (eq 21) and has a double-exponential decay with no maximum at $\tau > 0$ (Figure 7B). The lack of a delayed maximum reflects that there is no on-path intermediate toward product formation, as the initial state of each off-time in a turnover is ES after the substrate-assisted product dissociation (Scheme 3), and the state E is effectively an *off-path* "intermediate" toward product formation. (Note that, in this limiting case, only the *very first* turnover upon introducing substrate to the enzyme has the state E as the initial state for the off-time; however, this single event has no statistical significance in $f_{off}(\tau)$.)

(*iii*) $C_1 \neq 0$ and $C_2 \neq 0$. This is the general case and $f_{off}(\tau)$ then is a mix of behaviors of $f_{off}(\tau)_1$ and $f_{off}(\tau)_2$, whose relative contributions to $f_{off}(\tau)$ will depend on the relative magnitudes of the kinetic rate constants and the substrate concentration. Two special mathematical conditions exist in this general case, however, that can result in a simple single-exponential behavior of $f_{off}(\tau)$. Using eqs 20, 21, and 23, eq 22 can be rearranged to

$$f_{off}(\tau) = Ae^{(b+a)\tau} + Be^{(b-a)\tau} \tag{24}$$

where $A = [C_2k_2(a + b) + k_1k_2[S]] / 2a$ and $B = [C_2k_2(a - b) - k_1k_2[S]] / 2a$. Therefore, when $k_1[S] = -C_2(a + b)$, $A = 0$ and $f_{off}(\tau) = Be^{(b-a)\tau}$; when $k_1[S] = C_2(a - b)$, $B = 0$, and $f_{off}(\tau) = Ae^{(b+a)\tau}$; and both of these conditions will give a single-exponential behavior of $f_{off}(\tau)$. Experimentally, single-exponential decay behavior of waiting time distributions are normally used to argue for single-step reaction kinetics, but here we show that for complex reactions with parallel pathways, one of which even contains multiple steps, $f(\tau)$ can also be a single-exponential decay function at certain conditions.

IV.2.B. Rate of Product Formation: $\langle \tau_{off} \rangle^{-1}$**.** As for the product formation rate $\langle \tau_{off} \rangle^{-1}$ for a single enzyme molecule, from eq 22, we get

$$\langle \tau_{off} \rangle^{-1} = \frac{k_2[S]}{[S] + (k_{-1} + C_1k_2)/k_1}$$

$$= \frac{k_1k_2(k_3 + k_5)K_2[S]^2 + k_1k_2k_3[S]}{k_1(k_3 + k_5)K_2[S]^2 + [k_{-1}(k_3 + k_5)K_2 + k_3(k_1 + k_2K_2)][S] + k_3(k_{-1} + k_2)} \tag{25}$$

Although complex in expression due to the presence of multiple reaction pathways, $\langle \tau_{off} \rangle^{-1}$ still follows saturation kinetics with increasing substrate concentrations and saturate eventually to k_2 (Figure 7C).

IV.2.C. Randomness Parameter r_{off}**.** To describe the behavior of r_{off} for the modified Michaelis−Menten mechanism, we consider it in three different regimes in parallel to the discussion of its $f_{off}(\tau)$ (Section IV.2.A); the shape of $f_{off}(\tau)$ in these regimes determines the behavior of r_{off}.

(*i*) $C_1 = 1$ and $C_2 = 0$. $f_{off}(\tau)$ then reduces to $f_{off}(\tau)_1$ (eq 20), which has an exponential rise followed by an exponential decay with a delayed maximum (Figure 7A). Therefore, $r_{off} < 1$ at any [S], except at [S] = 0 or ∞ (Figure 7D).

(*ii*) $C_1 = 0$ and $C_2 = 1$. $f_{off}(\tau)$ then reduces to $f_{off}(\tau)_2$ (eq 21), which is a double-exponential decay function (Figure 7B). Therefore, $r_{off} > 1$ at any [S] except at [S] → ∞ (Figure 7D). (Note at [S] = 0, $r_{off} > 1$; see Appendix D.) In contrast to the τ_{on} reaction of this modified Michaelis−Menten mechanism, for which the double-exponential decay behavior of $f_{on}(\tau)$ comes from the presence of parallel pathways (Section IV.1), the double-exponential decay behavior of $f_{off}(\tau)$ here results from that the state E represents an *off-path* "intermediate" because the initial state is ES for each off-time after the substrate-assisted product dissociation (Scheme 3).

(*iii*) $C_1 \neq 0$ and $C_2 \neq 0$. In this regime, $f_{off}(\tau)$ is a mixture of $f_{off}(\tau)_1$ and $f_{off}(\tau)_2$ and its general form contains two exponentials with coefficients A and B (eq 24). At nonzero [S], $A > 0$ (Appendix E); thus, the sign of B decides the functional shape. If $B > 0$, $f_{off}(\tau)$ will be a double-exponential decay function and $r_{off} > 1$; if $B < 0$, $f_{off}(\tau)$ will then show an exponential rise followed by an exponential decay and $r_{off} < 1$; if $B = 0$, $f_{off}(\tau)$ reduces to a single-exponential decay function and $r_{off} = 1$. Figure 7E shows an exemplary plot of the [S] dependence of r_{off}: at different [S], r_{off} can be greater than 1 or smaller than 1 depending on the corresponding value of B and the cross point is where $B = 0$. Figure 7F shows three simulations of $f_{off}(\tau)$ corresponding to three different [S] in Figure 7E that give $f_{off}(\tau)$ double-exponential decay, single-exponential decay, or exponential-rise-followed-by-decay behaviors.

IV.3. Modified Michaelis−Menten Mechanism for Nanoparticle Catalysis. The modified Michaelis−Menten mechanism can also be useful for analyzing the single-turnover kinetics of nanoparticle catalysis. The Langmuir−Hinshelwood mechanism assumes a fast substrate adsorption equilibrium on the nanoparticle surface at all times (Scheme 2); however, if substrate adsorption−desorption is slow, the Langmuir−Hinshelwood mechanism is no longer applicable and the substrate adsorption−desorption needs to be treated explicitly. The modified Michaelis−Menten mechanism in Scheme 3 then provides an alternative, if we can assume as approximation one "effective" catalytic site that represents all the catalytic sites on the nanoparticle surface. Then, $f_{off}(\tau)$ and $\langle \tau_{off} \rangle^{-1}$ of eqs 22 and 25, as well as the associated r_{off}, can be used to analyze the single-turnover results of nanoparticle catalysis. k_2 in Scheme 3 will then represent the combined reactivity of all surface catalytic sites and can be related to γn_T in Scheme 2. The compromise of this approximation is the loss of explicit inclusion of the number of surface sites for considering the reactivity of a single nanoparticle.

V. Application of the Langmuir−Hinshelwood Mechanism to Oligomeric Enzymes

The classic Michaelis−Menten mechanism for enzyme catalysis is a one-site, one-substrate kinetic model. Many enzymes are oligomeric with multiple catalytic sites, however, such as the tetrameric enzyme β-galactosidase that has been studied at the single-molecule level.[4,12,55] Including the multiplicity of catalytic sites in the single-molecule kinetic formulism is thus desirable for oligomeric enzymes, because potential disorder in the number of active sites can play a role in the heterogeneous enzymatic dynamics revealed in single enzyme studies.[4,12,22]

The Langmuir−Hinshelwood mechanism explicitly includes the number of active sites in the kinetic formalism (Section II.1) and can thus be applied to oligomeric enzymes. The only prerequisite is that substrate binding/unbinding must be significantly faster than the catalytic conversion reaction in the catalytic cycle, so an equilibrium occupation of all active sites is established before a catalytic conversion occurs at one of the sites. An example that satisfies this prerequisite is the tetrameric enzyme β-galactosidase, which has been studied at the single-molecule level.[4,12,55]

We can then borrow the formulism of eq 6 of the Langmuir−Hinshelwood mechanism:

$$k_{app} = k_{cat} n \tag{26}$$

Here k_{app} is the apparent rate constant for an oligomeric enzyme to form *one* product at *one* of its active sites, k_{cat} is the *single-site* rate constant for catalytic conversion and n is the number of substrate molecules bound by the enzyme *at equilibrium*. Because the total number (n_T) of active sites of oligomeric enzymes is typically small, the relative fluctuation of the number of bound substrates can be large from one *instant* to another; however, the equilibrium occupation n is always described by its equilibrium binding isotherm and can be fractional at certain substrate concentrations. If the site−site interactions are insignificant among the monomers of the oligomeric enzyme, that is, monomers are independent of each other for substrate binding, n obeys the Langmuir isotherm: $n = n_T K[S]/(1 + K[S])$, where K is the binding equilibrium constant. We can then obtain expressions similar to eqs 12 and 13 to describe $f_{off}(\tau)$ and $\langle\tau_{off}\rangle^{-1}$ for oligomeric enzymes. If the site−site interactions are significant and there is cooperativity for substrate binding to the multiple active sites, alternative binding isotherms can then be used to describe n at different substrate concentrations. For example, if positive cooperativity exists for substrate binding, we can use a sigmoidal isotherm, such as the Monod−Wyman−Changeux model developed for the cooperative O_2 binding to hemoglobin,[1] to substitute the Langmuir isotherm to formulate the single-molecule kinetic equations.

Recent single-molecule enzyme studies have revealed large dynamic disorder, that is, temporal fluctuations of enzymatic rates, which were attributed to the fluctuations in k_{cat} caused by enzyme conformational dynamics.[3,4,7−9,22] The inclusion of the number of catalytic sites in the single-molecule kinetic equations offers an additional opportunity to evaluate possible causes of the dynamic disorder of oligomeric enzymes,[4,12,22] for example, temporal fluctuations of the number of available active sites in an oligomeric enzyme that can result from allosteric monomer−monomer interactions or from enzyme conformational dynamics.

VI. Concluding Remarks

In this paper, we have developed a theoretical formulism to describe the single-molecule kinetics of the heterogeneous catalysis by nanoparticle catalysts. We have described in detail the single-molecule kinetic theory of the Langmuir−Hinshelwood mechanism for the catalytic product formation reaction, which explicitly includes the multitude of surface sites on one nanoparticle, and considered two parallel product dissociation pathways that give complex single-molecule kinetics for the product dissociation reaction. We analyzed the statistical properties $f(\tau)$, $\langle\tau\rangle^{-1}$, and r of single-turnover waiting times at different kinetic limiting conditions and compared them with those of the Michaelis−Menten mechanism in enzyme catalysis. In light of the multiple product dissociation pathways in heterogeneous catalysis, we also derived the single-molecule kinetic equations for a modified Michaelis−Menten mechanism, which can be used to describe heterogeneous catalysis when the assumptions of the Langmuir−Hinshelwood mechanism break down. We further proposed that the formulism of the Langmuir−Hinshelwood mechanism for heterogeneous catalysis can be applied to single-molecule kinetic analysis of oligomeric enzymes that contain multiple catalytic sites.

As the Langmuir−Hinshelwood mechanism is a general mechanism for many heterogeneous catalysts,[51] we expect that our formulism will provide a general theoretical framework to understand single-molecule kinetics of heterogeneous catalysis. For example, our recent experimental work on the single-turnover catalysis of gold nanoparticles has revealed large dynamic disorder in their catalytic activity due to catalysis-induced surface restructuring dynamics of nanoparticles.[27] Surface restructuring dynamics can cause dynamic fluctuations in the number of catalytic sites and the reactivity of each site, both of which can result in dynamic changes in catalyst activity. The theoretical formulation of a kinetic mechanism here provides the foundation for analyzing such catalytic dynamics in heterogeneous catalysis at the single-molecule level.

Appendix

A. Derivation of the Probability Density Function $f_{on}(\tau)$ for the Langmuir−Hinshelwood Mechanism. For the Langmuir−Hinshelwood mechanism (Scheme 2), the reaction occurring during each on-time is either eq 14a or eq 14b. The single-molecule rate equations for these reactions are:

$$\frac{dP_{MS_{n-1}-P}(t)}{dt} = -(\gamma_1^0 + \gamma_3)P_{MS_{n-1}-P}(t) + \gamma_{-1}P_{MS_n-P}(t) \tag{A1a}$$

$$\frac{dP_{MS_n-P}(t)}{dt} = \gamma_1^0 P_{MS_{n-1}-P}(t) - (\gamma_{-1} + \gamma_2)P_{MS_n-P}(t) \tag{A1b}$$

$$\frac{dP_{MS_n}(t)}{dt} = \gamma_2 P_{MS_n-P}(t) \tag{A1c}$$

$$\frac{dP_{MS_{n-1}}(t)}{dt} = \gamma_3 P_{MS_{n-1}-P}(t) \tag{A1d}$$

where the $P(t)$'s are the probabilities of finding the nanoparticle in the corresponding states at time t; $\gamma_1^0 = \gamma_1[S]$ and is treated as a pseudofirst-order rate constant because [S] is time-independent in single-nanoparticle experiments. Equations A1a−d can be solved exactly using the initial conditions $P_{MS_{n-1}-P}(0) = 1$, $P_{MS_n-P}(0) = 0$,$P_{MS_n}(0) = 0$, and $P_{MS_{n-1}}(0) = 0$ with $t = 0$ being the onset of each on-time, and the constraint $P_{MS_{n-1}-P}(t) + P_{MS_n-P}(t) + P_{MS_n}(t) + P_{MS_{n-1}}(t) = 1$.

We can then consider the probability density function $f_{on}(\tau)$ of the on-time τ_{on}. τ_{on} is the time needed to complete either the reactions in eq 14a or the reaction in eq 14b. The probability of finding a particular τ is $f_{on}(\tau)\Delta\tau$, which is equal to the sum of (1) the probability for the nanoparticle to switch from the MS_n − P state to the MS_n state between τ and $\tau + \Delta\tau$ and (2) the probability for the nanoparticle to switch from the MS_{n-1} − P state to the MS_{n-1} state between τ and $\tau + \Delta\tau$. The probability of the first switching is $\Delta P_{MS_n}(\tau)$, which equals $\gamma_2 P_{MS_n-P}(\tau)\Delta\tau$. The probability of the second switching is $\Delta P_{MS_{n-1}}(\tau)$, which equals $\gamma_3 P_{MS_{n-1}-P}(\tau)\Delta\tau$. In the limit of infinitesimal $\Delta\tau$, we have

$$f_{on}(\tau) = \frac{dP_{MS_n}(\tau)}{d\tau} + \frac{dP_{MS_{n-1}}(\tau)}{d\tau} = \gamma_2 P_{MS_n-P}(\tau) + \gamma_3 P_{MS_{n-1}-P}(\tau) \tag{A2}$$

Solving eqs A1a−d for $P_{MS_n-P}(\tau)$ and $P_{MS_{n-1}-P}(\tau)$ using the initial conditions, we get

$$f_{on}(\tau) = \frac{1}{2\alpha}[Me^{(\beta+\alpha)\tau} + Ne^{(\beta-\alpha)\tau}] \quad \text{(A3)}$$

with $\alpha = \sqrt{(\gamma_1[S]+\gamma_{-1}+\gamma_2+\gamma_3)^2/4-(\gamma_1\gamma_2[S]+\gamma_{-1}\gamma_3+\gamma_2\gamma_3)}$, $\beta = -(\gamma_1[S] + \gamma_{-1} + \gamma_2 + \gamma_3)/2$, $M = \gamma_2\gamma_1[S] + \gamma_3\alpha + \gamma_3\beta + \gamma_3\gamma_{-1} + \gamma_3\gamma_2$, and $N = -\gamma_2\gamma_1[S] + \gamma_3\alpha - \gamma_3\beta - \gamma_3\gamma_{-1} - \gamma_3\gamma_2$. This equation is given as eq 15 in the main text.

B. Derivation of the Probability Density Function $f_{off}(\tau)$ for the Modified Michaelis−Menten Mechanism. For the modified Michaelis−Menten mechanism (Scheme 3), the relevant reactions in the off-time process are 3a and 3b; the single-molecule rate equations are:[3,28,31]

$$\frac{dP_E(t)}{dt} = -k_1^0 P_E(t) + k_{-1}P_{ES}(t) \quad \text{(B1a)}$$

$$\frac{dP_{ES}(t)}{dt} = k_1^0 P_E(t) - (k_{-1} + k_2)P_{ES}(t) \quad \text{(B1b)}$$

$$\frac{dP_{EP}(t)}{dt} = k_2 P_{ES}(t) \quad \text{(B1c)}$$

where k_1^0 ($= k_1[S]$) is a pseudofirst-order rate constant, and $P_E(t) + P_{ES}(t) + P_{EP}(t) = 1$. The procedure to obtain the probability density function of τ_{off}, $f_{off}(\tau)$, is similar to that described above. The probability of finding a particular τ is $f_{off}(\tau)\Delta\tau$, and this probability is equal to the probability for the enzyme to switch from the ES state to the EP state between $t = \tau$ and $\tau + \Delta\tau$, which is $\Delta P_{EP}(\tau) = k_2 P_{ES}(\tau)\Delta\tau$. In the limit of infinitesimal $\Delta\tau$,

$$f_{off}(\tau) = \frac{dP_{EP}(\tau)}{d\tau} = k_2 P_{ES}(\tau) \quad \text{(B2)}$$

Because of the presence of two product dissociation pathways, two sets of initial conditions are possible for solving eqs B1a−c: (*i*) $P_E(0) = 1$, and $P_{ES}(0) = P_{EP}(0) = 0$, if the product takes the direct dissociation pathway (reaction 3c, Scheme 3); or (*ii*) $P_E(0) = P_{EP}(0) = 0$, and $P_{ES}(0) = 1$, if the product takes the substrate-assisted dissociation pathway (reactions 3d and 3e). With the first set of initial conditions, we solve for $P_{ES}(\tau)$ and get

$$f_{off}(\tau)_1 = \frac{k_1 k_2[S]}{2a}[e^{(b+a)\tau} - e^{(b-a)\tau}] \quad \text{(B3)}$$

with $a = \sqrt{(k_1[S]+k_{-1}+k_2)^2/4-k_1k_2[S]}$, $b = -(k_1[S] + k_{-1} + k_2)/2$. With the second set of initial conditions, we get

$$f_{off}(\tau)_2 = \frac{k_2}{2a}[(a + b + k_1[S])e^{(b+a)\tau} + (a - b - k_1[S])e^{(b-a)\tau}] \quad \text{(B4)}$$

with the same a and b as above. Because both sets of initial conditions are possible, the probability density of τ_{off} should overall be a linear combination of eqs B3 and B4 for the modified Michaelis−Menten mechanism:

$$f_{off}(\tau) = C_1 f_{off}(\tau)_1 + C_2 f_{off}(\tau)_2 \quad \text{(B5)}$$

Here C_1 and C_2 are two weight coefficients representing the likelihoods of the two initial conditions, and $C_1 + C_2 = 1$. The magnitude of C_1 or C_2 should be proportional to the respective rate for the product to take the direct dissociation pathway or the substrate-assisted pathway. From eq 19, the product dissociation rate $\langle\tau_{on}\rangle^{-1}$ is equal to k_3 in the sole presence of the direct product dissociation pathway (i.e., $k_5 = K_2 = 0$) or to $k_5K_2[S]/(1 + K_2[S])$ in the sole presence of the substrate-assisted dissociation pathway (i.e., $k_3 = 0$). Therefore,

$$\frac{C_1}{C_2} = \frac{k_3(1 + K_2[S])}{k_5K_2[S]} \quad \text{(B6)}$$

With $C_1 + C_2 = 1$, we get

$$C_1 = \frac{k_3(1 + K_2[S])}{k_5K_2[S] + k_3(1 + K_2[S])} \quad \text{(B7a)}$$

$$C_2 = \frac{k_5K_2[S]}{k_5K_2[S] + k_3(1 + K_2[S])} \quad \text{(B7b)}$$

C. Randomness Parameter *r* for a Complex Reaction with Parallel Single-Step Reactions. For a complex reaction consisting of n parallel reaction steps, each being a single-step reaction with a rate constant k_n and all starting from the same state, the probability density function of the waiting time is $f(\tau) = (\Sigma_n k_n)\exp(-(\Sigma_n k_n)\tau)$. This $f(\tau)$ is obviously a single-exponential decay function; therefore, $r = 1$.

D. r_{off} of the Modified Michaelis−Menten Mechanism. For the modified Michaelis−Menten mechanism at the condition of $C_1 = 0$ and $C_2 = 1$, $f_{off}(\tau)$ (eq 22) reduces to $f_{off}(\tau)_2$ (eq 21). This limiting condition corresponds to the shutdown of the direct dissociation pathway (reaction 3c, Scheme 3), and the product can only dissociate via the substrate-assisted pathway (reactions 3d and 3e, Scheme 3). Therefore, the initial state for each off-time in the single-turnover trajectory is the ES state, except the *very first* turnover which has state E as the initial state upon introducing substrate to the enzyme. At $[S] = 0$, $f_{off}(\tau)_2$ reduces to $k_2e^{-(k_{-1}+k_2)\tau}$. Although this is a single-exponential decay function, it is not normalized, that is, $\int_0^\infty f_{off}(\tau)_2 d\tau = k_2/(k_{-1} + k_2) < 1$, leading to $r_{off} = 1 + 2k_{-1}/k_2 > 1$. The non-normalization of $f_{off}(\tau)_2$ at $[S] = 0$ results from that the forward reaction of 3a in Scheme 3 is eliminated at $[S] = 0$. Consequently, the E state becomes effectively a dead end of the catalysis; each time the reaction reaches state E, it leads to no completion of turnover and thus no measurement of a waiting time. The probability of reaching the E state after product dissociation is $k_{-1}/(k_{-1} + k_2)$, equal to $1 - \int_0^\infty f_{off}(\tau)_2 d\tau$.

E. Coefficient A in Eq 24. From Section IV.2, $A = k_2(C_2(a + b) + k_1[S])/2a$, where $C_2 = k_5K_2[S]/\{k_5K_2[S] + k_3(1 + K_2[S])\}$, $a = \sqrt{(k_1[S]+k_{-1}+k_2)^2/4-k_1k_2[S]}$, and $b = -(k_1[S] + k_{-1} + k_2)/2$. When $[S] = 0$, $A = 0$; when $[S] > 0$, $A > 0$. To prove the latter, we need to prove the following:

$$C_2(a + b) > -k_1[S] \quad \text{(E1)}$$

When $[S] > 0$, we have $0 < C_2 < 1$ and $a + b < 0$; then $C_2(a + b) > a + b$. Then to prove eq E1, we only need to show $a + b > -k_1[S]$, or equivalently

$$a > -b - k_1[S] = \frac{1}{2}(k_{-1} + k_2 - k_1[S]) \quad \text{(E2)}$$

If $[S]$ is large enough so that $(k_{-1} + k_2 - k_1[S])/2 \le 0$, the inequality in eq E2 can be met naturally because $a > 0$. If $[S]$ is not large and $(k_{-1} + k_2 - k_1[S])/2 > 0$, then the inequality in eq E2 is equivalent to

$$a^2 \ge \frac{1}{4}(k_{-1} + k_2 - k_1[S])^2 \quad \text{(E3)}$$

Using the expression for a, eq E3 can be rearranged to $k_{-1}k_1[S] \ge 0$, which is obviously true when $[S] > 0$.

Acknowledgment. We thank Cornell University, American Chemical Society Petroleum Research Foundation, and Cornell Center for Materials Research for financial support, and Professor Roger Loring for comments and suggestions.

References and Notes

(1) Fersht, A. *Structure and Mechanism in Protein Science: A Guide to Enzyme Catalysis and Protein Folding*; W. H. Freeman and Company: New York, 1998.

(2) Houston, P. L. *Chemical Kinetics and Reaction Dynamics*; Dover Publications: Mineola, NY, 2006.

(3) Lu, H. P.; Xun, L. Y.; Xie, X. S. *Science* **1998**, *282*, 1877.

(4) English, B. P.; Min, W.; van Oijen, A. M.; Lee, K. T.; Luo, G.; Sun, Y.; Cherayil, B. J.; Kou, S. C.; Xie, X. S. *Nat. Chem. Biol.* **2006**, *3*, 87.

(5) Edman, L.; FiSldes-Papp, Z.; Wennmalm, S.; Rigler, R. *Chem. Phys.* **1999**, *247*, 11.

(6) Edman, L.; Rigler, R. *Proc. Natl. Acad. Sci. U.S.A.* **2000**, *97*, 8266.

(7) De Cremer, G.; Roeffaers, M. B. J.; Baruah, M.; Sliwa, M.; Sels, B. F.; Hofkens, J.; De Vos, D. E. *J. Am. Chem. Soc.* **2007**, *129*, 15458–15459.

(8) Velonia, K.; Flomenbom, O.; Loos, D.; Masuo, S.; Cotlet, M.; Engelborghs, Y.; Hofkens, J.; Rowan, A. E.; Klafter, J.; Nolte, R. J. M.; de Schryver, F. C. *Angew. Chem., Int. Ed.* **2005**, *44*, 560.

(9) Flomenbom, O.; Velonia, K.; Loos, D.; Masuo, S.; Cotlet, M.; Engelborghs, Y.; Hofkens, J.; Rowan, A. E.; Nolte, R. J. M.; van der Auweraer, M.; de Schryver, F. C.; Klafter, J. *Proc. Natl. Acad. Sci. U.S.A.* **2005**, *102*, 2368.

(10) Antikainen, N. M.; Smiley, R. D.; Benkovic, S. J.; Hammes, G. G. *Biochemistry* **2005**, *44*, 16835.

(11) Smiley, R. D.; Hammes, G. G. *Chem. Rev.* **2006**, *106*, 3080.

(12) Gorris, H. H.; Rissin, D. M.; Walt, D. R. *Proc. Natl. Acad. Sci. U.S.A.* **2007**, *104*, 17680.

(13) Funatsu, T.; Harada, Y.; Tokunaga, M.; Saito, K.; Yanagida, T. *Nature* **1995**, *374*, 555.

(14) Ha, T. J.; Ting, A. Y.; Liang, J.; Caldwell, W. B.; Deniz, A. A.; Chemla, D. S.; Schultz, P. G.; Weiss, S. *Proc. Natl. Acad. Sci. U.S.A.* **1999**, *96*, 893.

(15) Lee, A. I.; Brody, J. P. *Biophys. J.* **2005**, *88*, 4303.

(16) Rondelez, Y.; Tresset, G.; Tabata, K. V.; Arata, H.; Fujita, H.; Takeuchi, S.; Noji, H. *Nat. Biotechnol.* **2005**, *23*, 361.

(17) Comellas-Aragonès, M.; Engelkamp, H.; Claessen, V. I.; Sommerdijk, N. A. J. M.; Rowan, A. E.; Christianen, P. C. M.; Maan, J. C.; Verduin, B. J. M.; Cornelissen, J. J. L. M.; Nolte, R. J. M. *Nature Nanotech.* **2007**, *2*, 635.

(18) Carette, N.; Engelkamp, H.; Akpa, E.; Pierre, S. J.; Cameron, N. R.; Christianen, P. C. M.; Maan, J. C.; Thies, J. C.; Weberskirch, R.; Rowan, A. E.; Nolte, R. J. M.; Michon, T.; van Hest, J. C. M. *Nature Nanotech.* **2007**, *2*, 226.

(19) Shi, J.; Dertouzos, J.; Gafni, A.; Steel, D.; Palfey, B. A. *Proc. Natl. Acad. Sci. U.S.A.* **2006**, *103*, 5775.

(20) Bagshaw, C. R.; Conibear, P. B. *Single Mol.* **2000**, *1*, 271.

(21) Zhang, Z.; Rajagopalan, P. T. R.; Selzer, T.; Benkovic, S. J.; Hammes, G. G. *Proc. Natl. Acad. Sci. U.S.A.* **2004**, *101*, 2764.

(22) van Oijen, A. M.; Blainey, P. C.; Crampton, D. J.; Richardson, C. C.; Ellenberger, T.; Xie, X. S. *Science* **2003**, *301*, 1235.

(23) Hanson, J. A.; Duderstadt, K.; Watkins, L. P.; Bhattacharyya, S.; Brokaw, J.; Chu, J.-W.; Yang, H. *Proc. Natl. Acad. Sci. U.S.A.* **2007**, *104*, 18055.

(24) Bagshaw, C. R.; Conibear, P. B. *Biochem. Soc. Trans.* **1999**, *27*, 33.

(25) Oiwa, K.; Eccleston, J. F.; Anson, M.; Kikumoto, M.; Davis, C. T.; Reid, G. P.; Ferenczi, M. A.; Corrie, J. E. T.; Yamada, A.; Nakayama, H.; Trentham, D. R. *Biophys. J.* **2000**, *78*, 3048–3071.

(26) Roeffaers, M. B.; Sels, B. F.; Uji-i, H.; De Schryver, F. C.; Jacobss, P. A.; De Vos, D. E.; Hofkens, J. *Nature* **2006**, *439*, 572.

(27) Xu, W.; Kong, J. S.; Yeh, Y.-T. E.; Chen, P. *Nat. Mater.* **2008**, *7*, 992.

(28) Kou, S. C.; Cherayil, B. J.; Min, W.; English, B. P.; Xie, X. S. *J. Phys. Chem. B* **2005**, *109*, 19068.

(29) Min, W.; English, B. P.; Luo, G.; Cherayil, B. J.; Kou, S. C.; Xie, X. S. *Acc. Chem. Res.* **2005**, *36*, 923.

(30) Min, W.; Gopich, I. V.; English, B. P.; Kou, S. C.; Xie, X. S.; Szabo, A. *J. Phys. Chem. B* **2006**, *110*, 20093.

(31) Xie, X. S. *Single Mol.* **2001**, *2*, 229.

(32) Cao, J. *Chem. Phys. Lett.* **2000**, *327*, 38.

(33) Cao, J. *J. Chem. Phys.* **2001**, *114*, 5137.

(34) Witkoskie, J. B.; Cao, J. *J. Chem. Phys.* **2004**, *121*, 6361.

(35) Qian, H.; Elson, E. L. *Biophys. Chem.* **2002**, *101*−*102*, 565.

(36) Gopich, I. V.; Szabo, A. *J. Chem. Phys.* **2006**, *124*, 154712.

(37) Xue, X.; Liu, F.; Ou-Yang, Z.-C. *Phys. Rev. E* **2006**, *74*, 030902.

(38) Xie, X. S. *J. Chem. Phys.* **2002**, *117*, 11024.

(39) Brown, F. L. H. *Phys. Rev. Lett.* **2003**, *90*, 028302.

(40) Vlad, M. O.; Moran, F.; Schneider, F. W.; Ross, J. *Proc. Natl. Acad. Sci. U.S.A.* **2002**, *99*, 12548.

(41) Zhou, Y.; Zhuang, X. *J. Phys. Chem. B* **2007**, *111*, 13600.

(42) Chemla, Y. R.; Moffitt, J. R.; Bustamante, C. *J. Phys. Chem. B* **2008**, *112*, 6025.

(43) Chaudhury, S.; Cherayil, B. J. *J. Chem. Phys.* **2007**, *127*, 105103.

(44) Cao, J.; Silbey, R. J. *J. Phys. Chem. B* **2008**, *112*, 12867–12880.

(45) Schnitzer, M. J.; Block, S. M. *Cold Spring Harbor Symp. Quant. Biol.* **1995**, *60*, 793.

(46) Svoboda, K.; Mitra, P. P.; Block, S. M. *Proc. Natl. Acad. Sci. U.S.A.* **1994**, *91*, 11782.

(47) Schnitzer, M. J.; Block, S. M. *Nature* **1997**, *388*, 386.

(48) Somorjai, G. A. *Introduction to Surface Chemistry and Catalysis*; Wiley-Interscience: New York, 1994.

(49) *Nanocatalysis*; Heiz, U., Landman, U., Eds.; Springer: Berlin, 2007.

(50) Ertl, G.; Knözinger, H.; Weitkamp, J. *Handbook of Heterogeneous Catalysis*; VCH: Weinheim, 1997.

(51) Satterfield, C. N. *Heterogeneous Catalysis in Practice*; McGraw-Hill Book Company: New York, 1980.

(52) Tschantz, W. R.; Furfine, E. S.; Casey, P. J. *J. Biol. Chem.* **1997**, *272*, 9989.

(53) Troutman, J. M.; Andres, D. A.; Spielmann, H. P. *Biochemistry* **2007**, *46*, 11299.

(54) Thomae, N. H.; Lakovenko, A.; Karlinin, A.; Waldmann, H.; Goody, R. S.; Alexandrov, K. *Biochemistry* **2001**, *40*, 268.

(55) Paige, M.; Fromm, D. P.; Moerner, W. E. *Proc. Soc. Photo-Opt. Instrum. Eng.* **2002**, *4634*, 92.

JP808240C